Direct imaging of domains in the $L_{\beta'}$ state of 1,2-dipalmitoylphosphatidylcholine bilayers

C.-W. Lee, R. S. Decca,* and S. R. Wassall
Department of Physics, Indiana University–Purdue University Indianapolis, 402 North Blackford Street, Building LD154, Indianapolis, Indiana 46202, USA

J. J. Breen†
Department of Chemistry, Indiana University–Purdue University Indianapolis, 402 North Blackford Street, Building LD326, Indianapolis, Indiana 46202, USA

(Received 24 January 2003; published 27 June 2003)

A near-field scanning optical microscope was used to study domain formation and evolution in single-component supported lipid bilayers in the gel ($L_{\beta'}$) state. Results on 1,2-dipalmitoylphosphatidylcholine (DPPC) bilayers on glass substrates at room temperature are presented. The domain structure is determined by means of the optical anisotropy of the sample, which arises because DPPC molecules are tilted at $\theta \sim 32°$ with respect to the bilayer normal [J. F. Nagle and S. Tristram-Nagle, Biochim. Biophys. Acta **1469**, 159 (2000)]. From the measurements we obtain the difference in the index of refraction for the directions parallel and perpendicular to the acyl chains of the lipid molecules, $\Delta n = 0.37 \pm 0.12$, in good agreement with calculated and measured values. Direct evidence of the existence of domains in the $L_{\beta'}$ state is provided. These domains, defined as the correlation of the tilt angle θ, are found to be 1–2 μm across. Furthermore, it was found that they are robust under single-lipid-molecule diffusion, remaining unchanged over periods of hundreds of minutes.

DOI: 10.1103/PhysRevE.67.061914 PACS number(s): 87.14.Cc, 78.20.Fm, 87.16.Dg, 87.64.Xx

I. INTRODUCTION

The complexity of cell membranes resides in their heterogeneous structure and composition. The concept of a homogeneously distributed mixture of phospholpids forming a bilayer into which proteins are embedded or to which they are attached [1] has recently been refined. There is now accumulating evidence that organized microdomains of specific lipid composition exist to provide a platform for membrane protein function [2,3]. Putative microdomain dimensions range from ~50 nm to several micrometers [4]. Matters are complicated further by the fact that the structural organization changes during protein activation [5]. Despite the extensive knowledge acquired, uncovering the relationship between membrane structure and function is far from completed. A common approach to improving the understanding of membranes is to study the behavior of individual constituents. In this regard, a significant effort has been dedicated to characterizing lipid bilayers [6], which account for ~50% of the membrane by weight [7].

Lipid bilayers not only play a fundamental structure-function role in cell membranes, they also exhibit a number of properties that make them interesting from a basic scientific point of view. Single-component lipid bilayers form a solidlike gel state at low temperature that, upon warming, turns into a liquid crystalline one when the acyl chains melt [8]. Although the details of the phase transition are lipid specific, it has been found that a variety of bilayers adopt several structurally different arrangements dependent upon temperature and hydration [6]. These bilayers could then be used as benchtop experiments for thermodynamic studies, providing examples of nematic, smectic and disordered liquid crystals.

A large number of experimental techniques have been successfully implemented to study synthetic lipid bilayers. Standard structural techniques such as NMR [9], and x-ray [6,10] and neutron diffraction [11] have been applied, but they are not local due to the intrinsic nature of the method or the difficulty of attaining adequate signal-to-noise ratio over the relevant time period. These techniques, nevertheless, have identified a number of properties of the bilayer, in the biologically relevant liquid crystalline phase and in the gel state. In particular, phosphatidylcholines containing two identical, saturated acyl chains are well characterized [6,8]. The structures formed by hydrated dipalmitoylphosphatidylcholine (DPPC) exemplify the complex phase behavior. A lamellar, crystalline subgel (L_c) phase is adopted after prolonged equilibration at ~0 °C. The gel state ($L_{\beta'}$), in which the acyl chains pack in a distorted hexagonal lattice, is adopted between 20 and 35 °C. In this phase the acyl chains are tilted an angle $\theta \sim 30°$ [6] relative to the normal to the bilayer plane. Upon further heating, the structure becomes corrugated in the plane of the bilayer to form the ripple phase (P'_β) between 35 and 41 °C, before transforming into the lamellar liquid crystalline (L_α) phase at higher temperatures. Relevant to this paper is the fact that the tilting of the acyl chains in the $L_{\beta'}$ phase manifests itself in the existence of optical anisotropy. This property has been exploited to measure the index of refraction perpendicular and parallel to the plane of the membrane, using ellipsometry [12] and coupled-plasmon waveguide resonance [13], over regions of several tens of square micrometers. It is natural to ask if θ is homogeneous throughout the sample, in both magnitude and polar orientation. X-ray data show that the magnitude is approxi-

*Electronic address: rdecca@iupui.edu
†Present address: Providence College, Providence, RI, USA.

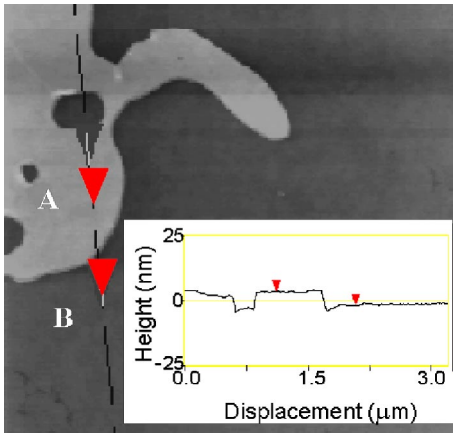

FIG. 1. Contact mode atomic force microscope image of a 3.2 $\times 3.2\ \mu m^2$ region of the edge of a DPPC sample. A shows a region where the lipid bilayer is formed, while B shows the underlying glass substrate. Inset: line cut across the lipid-glass interphase.

mately constant [6]. The experimental resolution in Ref. [6] indicates that order extends over regions with typical dimension larger than 290 nm. A more precise measurement of the size and shape of these domains, however, is an outstanding question.

The superior spatial resolution of near-field scanning optical microscopy (NSOM) [14] compared to conventional far-field optical approaches has attracted application to biophysical research [15]. Shiku and Dunn [16] employed NSOM observation of fluorescently labeled probes incorporated into lipid monolayers to explore domain formation on the nanometer scale. In an earlier study we demonstrated the potential of the approach to track the lateral diffusion of a single fluorescently labeled lipid molecule in a membrane [17]. The objective of this paper is to investigate the lateral organization of lipid bilayers in the gel phase without the incorporation of an extrinsic probe. Instead, the local polar orientation of lipid molecules and its effect on the optical properties of lipid bilayers are investigated on a topography-free system by means of a NSOM. The lateral organization of a pure DPPC membrane in the $L_{\beta'}$ state is imaged with a spatial resolution of $\sim$100 nm, providing direct observation of domains.

II. EXPERIMENTAL DETAILS

A. Sample preparation and characterization

Supported bilayers of DPPC were prepared by fusion of sonicated unilamellar vesicles (SUVs) onto a glass surface [18]. SUVs (1–5 mg/ml lipid) were made in 70 mM NaCl/20 mM NaH_2PO_4 (pH 7) and a drop ($\sim$50 μl) was deposited onto a glass slide. The sample was incubated overnight at $\sim$4 °C, followed by another 2 h at $\sim$60 °C. Excess lipid and buffer were then washed off. The same procedure was also applied to prepare supported bilayers of DPPC in the presence of 30 mol % cholesterol. For atomic force microscopy (AFM) the bilayers were transferred to a fluid cell, while for NSOM they were kept in a chamber under 100% relative humidity. All measurements were performed at

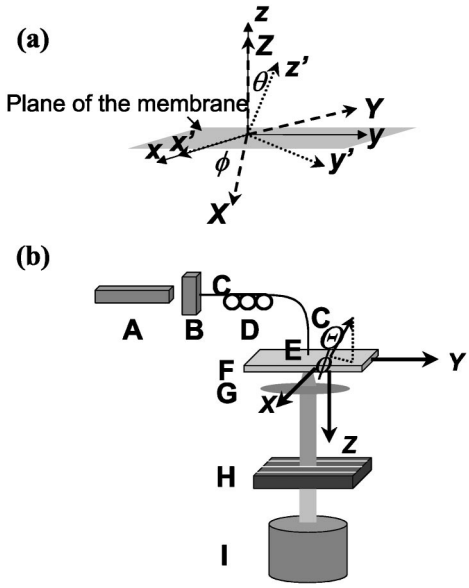

FIG. 2. (a) Relevant coordinate systems associated with the membrane and light propagation. The plane of the membrane is xy (coincident with XY), with z (and Z) perpendicular to the membrane. The XYZ coordinate system is obtained through a rotation of xyz by ϕ about z. $x'y'z'$ is obtained through a θ rotation about x. (b) Schematic of the experimental setup: (A) He-Ne laser; (B) laser-to-fiber coupler; (C) single mode optical fiber; (D) fiber polarization controller; (E) NSOM probe; (F) sample on piezo driven stage; (G) microscope objective, 0.7 NA; (H) linear polarizer (the lines indicate the direction of the polarizer); (I) detector.

$\sim$20 °C, in the $L_{\beta'}$ state. A contact mode AFM image of a pure DPPC sample is shown in Fig. 1. The image was chosen to show regions where the glass substrate is covered by the DPPC bilayer membrane (noted as A) and regions where it is not (labeled as B). In the regions A of all samples the fluctuations in the topography were observed to be ± 0.1 nm. From this value and the difference in height between regions A and B, the height of the membrane is determined to be $t = 5.3 \pm 0.1$ nm. This value is in very good agreement with the thickness of a single DPPC bilayer in the gel state [6].

B. Experimental setup and methods

As aforementioned [12,13], optical contrast in the $L_{\beta'}$ state arises from the anisotropic index of refraction of phospholipid bilayers [13]. In this paper, the lipid bilayer is considered as a uniaxial optical crystal, with principal optical axis along the direction of the acyl chains in the lipid molecule. In DPPC, this direction is known to be $\theta \sim 32°$ [6] with respect to the perpendicular to the plane of the membrane. The difference in polarizability of the molecules along the acyl chains and perpendicular to them gives rise to a difference between the respective indexes of refraction $n_{\|}$ and $n_{\perp}$. Considering the membrane to lie on the xy plane [see Fig. 2(a)], linearly polarized electromagnetic radiation of wavelength λ propagating along $\hat{z}$ and polarized along $\hat{x}$ will be retarded with respect to that polarized along $\hat{y}$ by

$$\Delta\varphi=\frac{2\pi}{\lambda}t(n_e-n_o)=\frac{2\pi}{\lambda}tn_\perp\left|1-\left[\frac{\tan^2\theta+1}{(\tan\alpha)^2+1}\right]^{1/2}\right|, \tag{1}$$

where $\hat{y}$ coincides with the direction of the projection of the acyl chains on the xy plane. In Eq. (1) $n_o(n_e)$ is the effective index of refraction for the ordinary (extraordinary) ray, $\tan\alpha=\eta\tan\theta$, $\eta=n_\perp/n_\parallel$. The last part of Eq. (1) is valid for $\theta\neq 0°$ Due to the small thickness of the membrane, the ordinary and extraordinary rays are not distinguishable by the collection optics. Under these circumstances, the bilayer acts as a retarder with Jones matrix [19] $\mathcal{M}_s=\left(\begin{smallmatrix}e^{i\Delta\varphi} & 0\\ 0 & 1\end{smallmatrix}\right)$, where a constant phase difference has been omitted.

The experiment is performed with light linearly polarized along a direction $\hat{X}$ in the xy plane. The direction of the polarization forms an angle ϕ with the $\hat{x}$ axis, and the light transmitted through the sample is, in general, elliptically polarized. For a homogeneous sample, analysis of the degree of ellipticity yields a measurement of ϕ and $n_\parallel$ when $n_\perp$ and θ are known, as described below.

Figure 2(b) shows a schematic of the experimental setup. Light from a He-Ne laser is coupled into a single-mode optical fiber. Using the universal polarizer, light coming out of the NSOM probe is made as close to linearly polarized as possible. Aperture NSOM probes, either 100 nm Al coated or uncoated, were used to obtain images of the DPPC membrane. The results did not show any qualitative differences, except for the obvious loss of spatial resolution for the uncoated probes. It was found that a polarization ratio $(\vec{E}\cdot\hat{X}/\vec{E}\cdot\hat{Y})^2\sim 70$ can be systematically achieved [20] for both probes. The tip-to-sample separation, controlled with a tuning fork based shear force system [17,21], was kept at $\sim$20–30 nm. Hence, light coming out of the NSOM probe may be considered to be essentially elliptically polarized [20,22]. The analyzer is a linear polarizer oriented along $\hat{Y}$ such that when no sample is present the signal level at the detector is minimum.

Under these conditions, the electromagnetic radiation on the detector has an amplitude of the electric field given by

$$\vec{E}_0=\begin{pmatrix}E_X^D\\ E_Y^D\end{pmatrix}=\begin{pmatrix}0 & 0\\ 0 & 1\end{pmatrix}\times\begin{pmatrix}\cos\phi & -\sin\phi\\ \sin\phi & \cos\phi\end{pmatrix}\times\begin{pmatrix}e^{i\Delta\varphi} & 0\\ 0 & 1\end{pmatrix}\times\begin{pmatrix}\cos\phi & \sin\phi\\ -\sin\phi & \cos\phi\end{pmatrix}\times\begin{pmatrix}E_X^P\\ E_Y^P\end{pmatrix}, \tag{2}$$

where $E_j^D(E_j^P)$ is the j component of the amplitude of the electric field at the detector (probe). The Jones matrix of the sample in Eq. (2) has been rotated to be represented on the XY system, and $\left(\begin{smallmatrix}0 & 0\\ 0 & 1\end{smallmatrix}\right)$ is the Jones matrix of the analyzer. From Eq. (2), the normalized irradiance at the detector is found to be

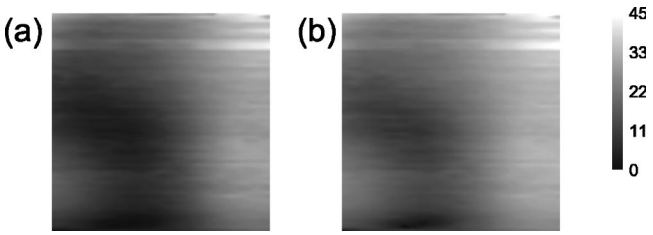

FIG. 3. (a) NSOM image of a 3.2×3.2 μm^2 region of a DPPC sample. (b) Polar orientation ϕ of DPPC molecules on the XY plane.

$$\frac{I(\phi,\Delta\varphi)-I(0,\Delta\varphi)}{I(0,\Delta\varphi)}=\sin^2(2\phi)\sin^2\left(\frac{\Delta\varphi}{2}\right)\left[\left(\frac{E_X}{E_Y}\right)^2-1\right]+\sin(2\phi)\sin\Delta\varphi\left(\frac{E_X}{E_Y}\right). \tag{3}$$

Equation (3) shows that for $\phi=0$ or $90°$ the irradiance is a minimum. Also, regions of the sample that present maximum transmission have the projection of the acyl chains on the xy plane oriented at $45°$ or $135°$ with respect to the direction of the analyzer. For the case of maximum transmission the value of $\Delta\varphi$ is obtained from the data using Eq. (3), and using Eq. (1) $n_\parallel$ is obtained if both $n_\perp$ and θ are known.

III. RESULTS

Figure 3(a) shows typical raw data obtained with the NSOM while scanning a 3.2×3.2 μm^2 area of the DPPC bilayer. The contrast in Fig. 3(a), defined as $\mathcal{K}=I(45°)/I(0°)-1$, is $\sim$3.5%, and the noise is $\mathcal{N}_e=0.15\mathcal{K}$. These figures for noise and contrast show little variation among the pure DPPC samples measured. The image was obtained and then the tip was brought back to the point of minimum transmission. At this particular location the analyzer was rotated to find $(E_X/E_Y)^2=65\pm2$. As described in Sec. II B, the maximum transmission was used to define $\phi=45°$, and from here

$$\frac{I(45°,\Delta\varphi)-I(0,\Delta\varphi)}{I(0,\Delta\varphi)}\simeq\frac{x_p^2}{4}+x_p, \tag{4}$$

where $x_p=(E_X/E_Y)\Delta\varphi$, and the facts that $(E_X/E_Y)^2\gg1$, $\Delta\varphi\ll 1$ were used. The repetition of this process for several regions of the sample showing maximum transmission and several different samples allows us to get $\Delta n'=n_e-n_o=0.08\pm0.02$ and, using Eq. (1), $\theta=32°$ and $n_\perp=1.40$ [13], $n_\parallel-n_\perp=0.37\pm0.12$. The value of $n_\perp=1.40$ is calculated from the polarizability of the molecule (see Ref. [13]). Measured values of $\Delta n'$ range from 0.03 [12] to 0.055 [13], yielding in this last case $\Delta n=0.29$ [13], which barely overlaps with the measured Δn from this paper. The previous underestimation of Δn arises from the averaging over different orientations, as described below.

Once the value of x_p has been determined for a given sample-NSOM probe set, Eq. (3) can be used to find ϕ, i.e., the direction of the projection of the acyl chains on the xy plane. These results are plotted in Fig. 3(b). Since the irradi-

ance is symmetric with respect to $\phi = 45°$, the directions in Fig. 3(b) are chosen to cover only the $\phi' \in [0,45°]$ range. The results shown in Fig. 3 are the most significant of this paper. They provide direct observation of domains existing in the $L_{\beta'}$ phase of DPPC. These domains are better associated with a correlation length, akin to what is observed in systems described by an xy model [23]. As can be observed, the orientational order varies smoothly as a function of position, not showing any sign of grain boundaries, a common trend in all samples investigated. At the present time the underlying mechanism for domain formation in the gel state remains unclear.

The autocorrelation function of the angular orientation,

$$\Phi(x,y) = \int \int \phi'(x+x',y+y')\phi(x',y')dx'dy', \quad (5)$$

where the integral is done over the area of the image, is used to define the characteristic size of a domain. The full width at half maximum of the distribution is defined as the size of the domain ξ. In all the samples investigated it was found that $\xi \simeq 1$ μm. The relatively short correlation length ξ partially explains why the value of Δn is larger than those found in previous work [12,13]: while the use of NSOM allows one to obtain a value of Δn within a domain, an average over several domains with $\Delta n'$ ranging from 0 to ~ 0.08 was determined with ellipsometry [12] and coupled-plasmon waveguide resonance [13].

It could be argued that the contrast in Fig. 3(a) is an artifact caused by interference between the NSOM probe, the sample, and the substrate, or that the thickness of the sample is not homogeneous. While the latter possibility is ruled out by AFM measurements (see Fig. 1), some care has to be exercised when dealing with the former. With this aim, samples with no anisotropy but otherwise as similar as possible to the DPPC supported bilayer were prepared. At room temperature DPPC containing 30 mol % cholesterol is entirely in the liquid ordered phase (l_o), with the acyl chains perpendicular to the membrane [24]. In this configuration the optical axis of the material is parallel to the propagation of the light and no birefringence should be observed. An image of such a sample is shown in Fig. 4, where $\mathcal{K} \lesssim \mathcal{N}$. Hence, within the experimental resolution, $x_p = 0$ from Eq. (4), and $\Delta n' = 0$.

As a final measurement, the stability of the domains observed in Fig. 3(a) was characterized. It is known that in supported bilayers of DPPC in the $L_{\beta'}$ state the lateral diffusion coefficient of lipid molecules is $D \sim 10^{-16}$ m^2/s [25]. In the time it takes to obtain an image (~ 10 min) a molecule is displaced by $r \simeq 0.5$ μm. If the molecules diffuse conserving their spatial orientation, the domains will change on the same time scale. This scenario, however, would involve a large elastic energy, since all the molecules in the sample would have to be diffusing coherently. On the other hand, the individual diffusion of each molecule where it adjusts to the local orientation would produce an uncorrelated diffusion among the molecules, leaving the pattern unchanged. Figure 5 shows the first and the last of a series of images taken over a time span of 3 h. It can be seen that the main features of the image are preserved, although a very slow creep of the domains may be present. The average speed of the $\overline{AA'}$ line, defined between two points where $\mathcal{K}/\mathcal{K}_{MAX} = \frac{1}{2}$, is $v < 1.5 \times 10^{-10}$ m/s.

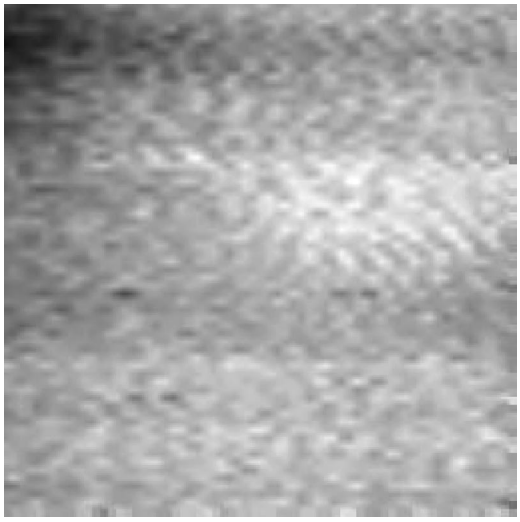

FIG. 4. NSOM image of a 3.2×3.2 μm^2 region of a DPPC:30 mol % cholesterol sample.

IV. CONCLUSIONS

An implementation of a NSOM to measure the local optical activity in lipid bilayers was presented. It was shown that the NSOM can be used to measure the difference in the indexes of refraction in the gel state of lipid bilayers. In particular, these measurements were carried out on a system whith no topographic contrast. The measurements described

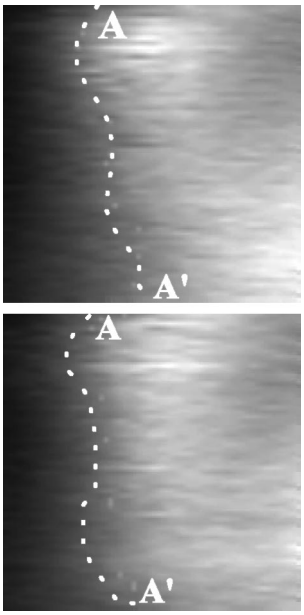

FIG. 5. NSOM images of a 3.2×3.2 μm^2 region of a DPPC sample. These images are the first and last of a time sequence covering a 3 h span (see text). The lines are defined on a row by row basis at the contrast half tone.

in the paper require the existence of an anisotropic index of refraction on the plane of the membrane over ~ 100 nm. Consequently, the existence of a gel phase is imperative. It is possible, however, to extend the the method to a gel-liquid crystalline mixture. In this scenario the gel fraction would provide optical contrast while the liquid crystalline fraction would not.

The direct observation of domains ~ 1 μm across, robust under diffusion of lipid molecules, opens up the possibility of studying $\xi(T)$. Knowing the correlation length as a function of temperature should allow the determination of the contribution of domain formation to the free energy of the membrane [23]. The smooth transition in the polar orientation, with no grain boundaries observed, suggests the possibility of describing the system within an xy model. Furthermore, although clear evidence of the existence of relatively small domains in the gel state has been presented, identification of the instability that induces their formation remains to be obtained.

ACKNOWLEDGMENT

R.S.D. acknowledges financial support from the Petroleum Research Foundation through ACS-PRF Grant No. 37542-G.

[1] S. J. Singer and G. L. Nicholson, Science **175**, 720 (1971).
[2] B. K. Jacobson, E. D. Sheets, and R. Simson, Science **268**, 1441 (1995).
[3] K. Simons and E. Ikonen, Nature (London) **387**, 569 (1997).
[4] R. G. W. Anderson and K. Jacobson, Science **296**, 821 (2002).
[5] W. Dowhan, Annu. Rev. Biochem. **66**, 199 (1997).
[6] J. F. Nagle and S. Tristram-Nagle, Biochim. Biophys. Acta **1469**, 159 (2000).
[7] R. B. Gennis, *Biomembranes* (Springer-Verlag, New York, 1989).
[8] R. Koynova and M. Caffrey, Biochim. Biophys. Acta **1376**, 91 (1998).
[9] M. F. Brown, *Biological Membranes: A Molecular Perspective from Computation and Experiment*, edited by K. M. Merz and B. Roux (Birkhäuser, Boston, 1996), pp. 175–252.
[10] W.-J. Sun, R. M. Suter, M. A. Knewtson, C. R. Worthington, S. Tristram-Nagle, R. Zhang, and J. F. Nagle, Phys. Rev. E **49**, 4665 (1994).
[11] J. Katsaras, Biophys. J. **75**, 2157 (1998).
[12] D. den Engelsen, Surf. Sci. **56**, 272 (1976).
[13] Z. Salamon and G. Tollin, Biophys. J. **80**, 1557 (2001).
[14] *Optics at the Nanometer Scale*, Vol. 319 of *Advanced Study Institute, NATO Series E: Applied Physics*, edited by M. Nieto-Vesperinas and N. García (Kluwer, Dordrecht, 1996).
[15] M. Edidin, Traffic **2**, 797 (2001).
[16] H. Shiku and R. C. Dunn, J. Microsc. **194**, 461 (1998).
[17] R. S. Decca, C.-W. Lee, S. Lall, and S. R. Wassall, Rev. Sci. Instrum. **73**, 2675 (2002).
[18] P. S. Cremer and S. G. Boxer, J. Phys. Chem. B **103**, 2554 (1999).
[19] F. L. Pedrotti and L. S. Pedrotti, *Introduction to Optics*, 2nd ed. (Prentice-Hall, Upper Saddle River, NJ, 1993).
[20] R. S. Decca, H. D. Drew, and K. L. Empson, Appl. Phys. Lett. **70**, 1932 (1997).
[21] K. Karrai and R. D. Grober, Appl. Phys. Lett. **66**, 1842 (1995).
[22] R. D. Grober, T. Rutherford, and T. D. Harris, Appl. Opt. **35**, 3488 (1996).
[23] P. M. Chaikin and T. C. Lubensky, *Principles of Condensed Matter Physics* (Cambridge University Press, Cambridge, 1995).
[24] J. H. Davis, in *Cholesterol in Membrane Models*, edited by L. Finegold (CRC Press, Boca Raton, FL, 1993), pp. 67–135.
[25] L. K. Tamm and H. M. McConnell, Biophys. J. **47**, 105 (1983).